

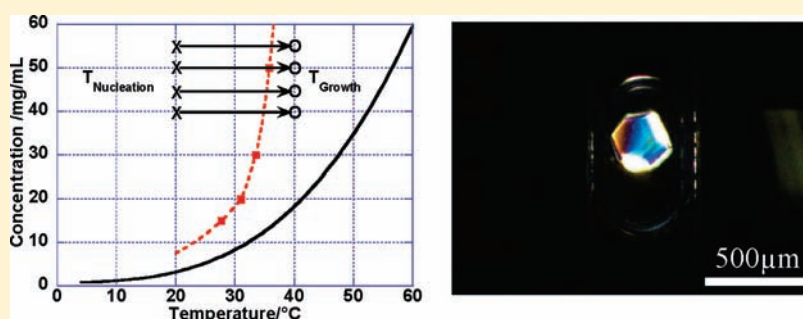
Using Microfluidics for Fast, Accurate Measurement of Lysozyme Nucleation Kinetics

Published as part of a virtual special issue of selected papers presented at the 9th International Workshop on the Crystal Growth of Organic Materials (CGOM9).

M. Ildefonso, N. Candoni, and S. Veessler*

Centre Interdisciplinaire de Nanoscience de Marseille CINAM—CNRS, Campus de Luminy, Case 913, F-13288 Marseille Cedex 09, France, In association with Marseille Universities

ABSTRACT:



Here we measure lysozyme nucleation kinetics using an easy-to-use and simply constructed microfluidics setup previously described. We confirm that microfluidics is a direct, accurate, and fast method to measure nucleation frequency using only a few milligrams of molecules. Moreover, our microfluidics setup, by diminishing crystallizer volumes, increases the experimental supersaturation range accessible and can be applied to all water-soluble molecules.

1. INTRODUCTION

In this paper, we focus on nucleation, which plays a fundamental role in crystallization processes, notably determining the physical properties of crystals, including crystal size distribution and phases. The control of nucleation kinetics is a real challenge in many scientific fields, for instance in biology and pharmacology. Although a great deal is known about crystal growth, considerably less is known about crystal nucleation because of the difficulty of obtaining reliable kinetic data. Reliable data are difficult to obtain because nucleation is a stochastic phenomenon and, therefore, an accurate determination of nucleation kinetics requires a large sample of independent nucleation events. With a view to generating kinetic data, microfluidics offers an interesting potential for the control and the study of nucleation, by enabling the number of experiments to be increased and the quantity of molecules to be decreased.^{1–4} Here, we employ an easy-to-use and simply constructed microfluidics setup developed by Salmon,^{5,6} which we had previously adapted for nucleation research.⁷ The hundreds of droplets generated in the microfluidics chip yields a large sample of independent nucleation events. We then investigated the nucleation kinetics of hen-egg white lysozyme (HEWL) using the double pulse technique.^{8–10}

2. MATERIALS AND METHODS

2.1. Protein Solutions. HEWL (molecular weight = 14.6 kDa and isoelectric point = 11.2) was purchased from Sigma (batch

057K7013 L 2879) and used without further purification. The purity of lysozyme was checked by molecular sieving. A suitable amount of lysozyme was dissolved in pure water (ELGA UHQ reverse osmosis system) to obtain the stock solutions required. A 1.4 M NaCl solution was also prepared. The different solutions were buffered with 80 mM acetic acid, adjusted to pH = 4.5 with NaOH (1 M) and filtered through 0.22 μm Millipore filters. The pH was checked with a pH meter (Schott Instrument, Prolab 1000) equipped with a pH microelectrode. Lysozyme concentrations were checked by optical density measurements (Biochrom, Libra S22) using an extinction coefficient of 2.64 mL cm⁻¹ mg⁻¹ at 280 nm. In all the crystallization experiments hereunder, the NaCl concentration was fixed at 0.7 M at pH = 4.5.

2.2. Droplet Generation and Storage. The basic microdevice design is fabricated in poly(dimethylsiloxane) (PDMS) by using soft-lithographic techniques (Figure 1a); the construction and procedure were previously described.^{5,7} Protein and salt solutions were injected into the 500 μm -channel of the chip at a rate of 300 $\mu\text{L}/\text{h}$ with syringe pumps (Bioseb BS800) and thus mixed by diffusion. Droplets were generated at the intersection between the silicone oil (Sigma oil AP 100, viscosity 940cSt) and aqueous streams using the flow focusing method^{11,12} (Figure 1b). Up to

Received: October 27, 2010

Revised: March 4, 2011

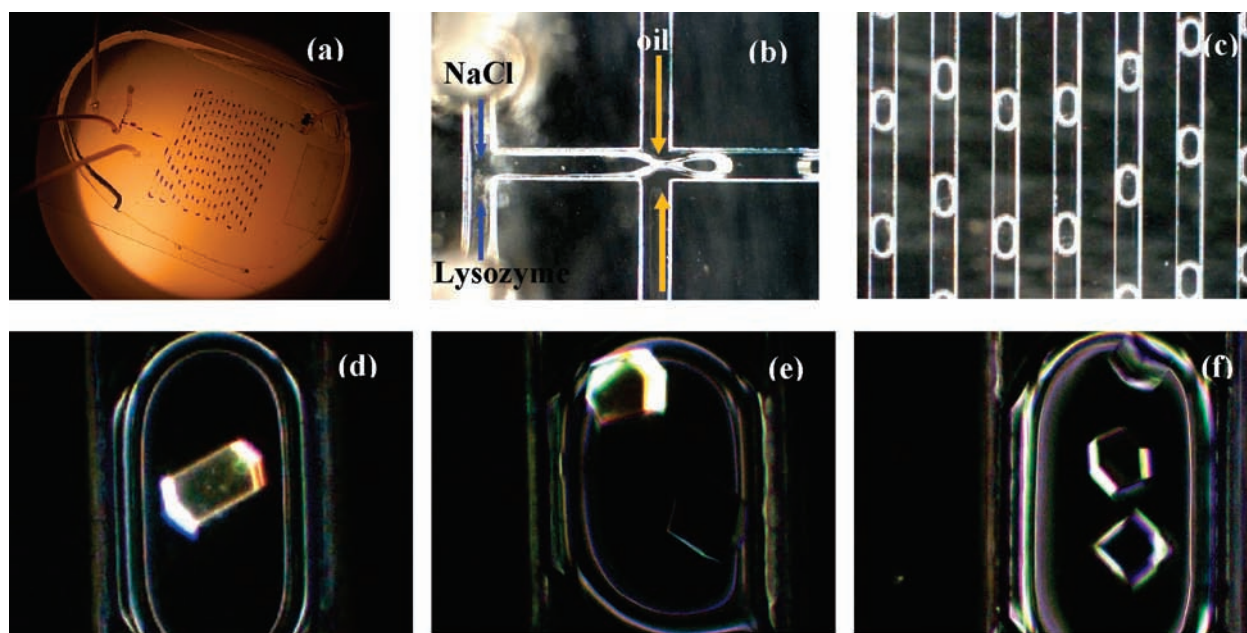


Figure 1. (a) Image of the device, (b) zoom of the inlets of the plug factory showing droplet formation, (c) image of the stored droplets, and (d–f) examples of lysozyme droplets observed after 20 h, at $T_{\text{nucleation}} = 20\text{ }^{\circ}\text{C}$ and $T_{\text{growth}} = 40\text{ }^{\circ}\text{C}$ (channel width $500\text{ }\mu\text{m}$).

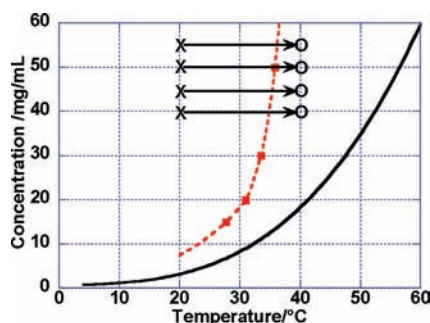


Figure 2. Tetragonal lysozyme (0.7 M NaCl, pH = 4.5) solubility versus temperature according to Cacioppo et al.¹⁷ and metastable zone curves according to Ildefonso et al.;⁷ lines improve legibility. Points (\times) and (\circ) indicate nucleation and growth conditions, respectively. Arrows represent the experimental path in the phase diagram.

200 droplets were stored in one chip (Figure 1c); each droplet had a volume of 250 nL with a volume polydispersity of a few percent.^{6,13} Using the plug factory zone (Figure 1b) for the generation of droplets,⁷ several chips could be filled with the same chemical composition. Then the crystals that had nucleated in each drop were observed and counted under a stereomicroscope (Wild Makroskop) equipped with a CCD camera (imaging source, DFK 31BF03). During observation, the device was thermostatted by Peltier elements (Anacrismat, France). Typical images are shown in Figure 1d–f.

2.3. Determination of Nucleation Rate. We used the double pulse technique,^{8–10} allowing direct determination of the steady-state rate of primary nucleation. At the beginning of an experiment, the solution was loaded into the chip at a temperature chosen to prevent nucleation of crystals, T_{growth} . In order to obtain nucleation, we lowered the temperature to a selected $T_{\text{nucleation}}$. After a period of Δt (nucleation time), temperature was raised from $T_{\text{nucleation}}$ to T_{growth} (Figure 2). At T_{growth} supersaturation was at a level where the nucleation rate was practically zero, but the crystals already formed

could grow to detectable dimensions. The use of this method allows decoupling of nucleation and the ensuing growth. After the growth stage, the crystals nucleated at $T_{\text{nucleation}}$ during Δt are counted. After plotting the average number of crystals nucleated as a function of the Δt , the steady state nucleation rate is determined as represented by the slope of the straight line plotted. We fitted the experimental crystal distribution with a Poisson law, as previously reported by Galkin and Vekilov.⁹ For all experimental conditions, here four chips were filled with the same solution, using the procedure described in section 2.1, allowing four nucleation times to be tested simultaneously. Chips were stored at $T_{\text{nucleation}}$ in an incubator; because temperature could be reached within 1 min, we used the shortest Δt of 15 min to avoid uncertainties due to T changes.⁹ Moreover, evaporation of water through the PDMS layer is negligible in our experiments because it was previously shown that aqueous droplets stored at $60\text{ }^{\circ}\text{C}$ in the same device decrease by 10% in about 4 h.¹⁴ It must be noted that for long storage time at $40\text{ }^{\circ}\text{C}$ if a second nucleation wave occurred, we would observe crystals of different sizes in the same droplet, and this is not the case here; see Figure 1e and f, for instance.

3. RESULTS AND DISCUSSION

3.1. Experimental Parameters. With the double pulse technique, there are four parameters to adjust: $T_{\text{nucleation}}$, T_{growth} , concentration, and nucleation time. We chose a nucleation temperature of $20\text{ }^{\circ}\text{C}$, in order to compare our data with the data from the literature.^{9,15} Since the T_{growth} needs to be in the metastable zone, we chose $40\text{ }^{\circ}\text{C}$ (Figure 2), having previously measured the metastable zone width for lysozyme under the same conditions with the same microfluidics setup.⁷ Preliminary measurements showed that the average number of crystals per droplet after 20 h at $20\text{ }^{\circ}\text{C}$ is very low at 20 and 30 mg/mL. Therefore, we conducted experiments between 40 and 55 mg/mL. To test metastability, we also performed experiments at $40\text{ }^{\circ}\text{C}$, i.e. $\Delta t = 0$, for all experimental conditions. The constraint in choice of the nucleation time is the number of crystals

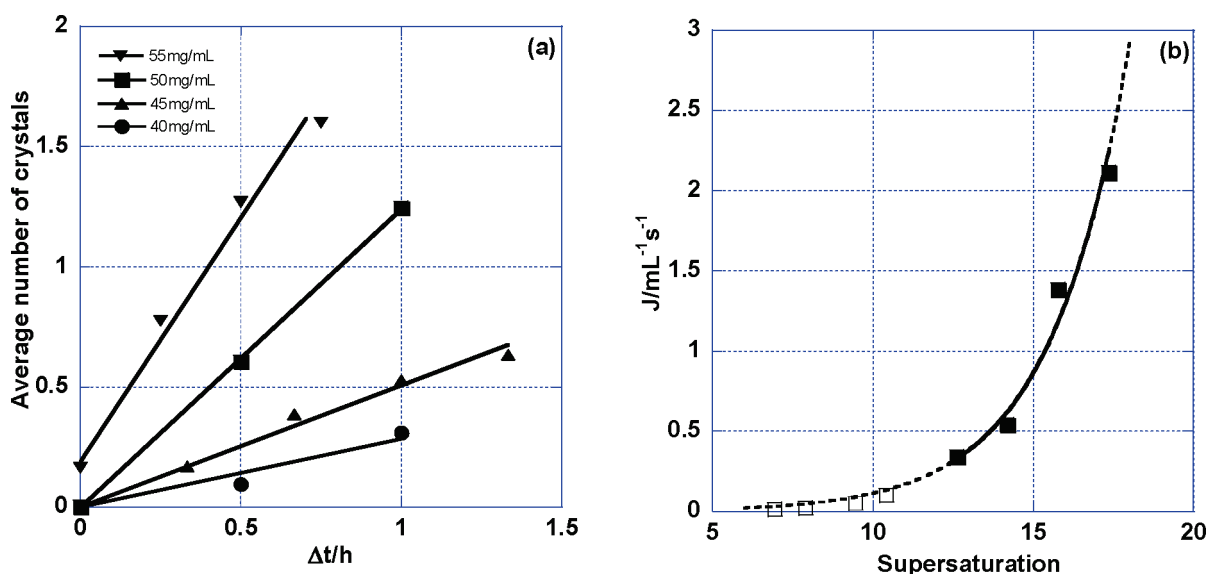


Figure 3. (a) Average number of lysozyme crystals nucleated in one droplet versus nucleation time (NaCl = 0.7 M and pH = 4.5), (b) primary nucleation rate vs supersaturation, at 20 °C, (■) from the slope of the straight lines of Figure 3a and (□) data, at 12.6 °C, $C_s = 1.6$ mg/mL, from Galkin and Vekilov.¹⁸

Table 1. Average Number of Lysozyme Crystals Nucleated in One Droplet^a

protein conc (mg/mL)	avg no. lysozyme crystals at the following nucleation times							
	0 min	15 min	20 min	30 min	40 min	45 min	1 h	1 h 20 min
40	0			0.094 (3.1)			0.308 (1.7)	
45	0		0.170 (2.3)		0.385 (1.5)		0.528 (1.9)	0.633 (1.3)
50	0			0.606 (1.4)		1.245 (1.8)		
55	0.164 (4.0)	0.776 (2.0)		1.269 (1.7)		1.600 (1.3)		

^aThe deviation in % is given in parentheses.

nucleated per droplet. Due to the droplet volume, here 250 nL, the lysozyme concentration could not be considered constant if the nucleation time was too long, explaining the saturation effect observed. In practice, the average number of crystals per droplet no longer varied linearly with nucleation time. We therefore chose to use 15 min < Δt < 2 h (Figure 3a).

3.2. Primary Nucleation Rates. Table 1 summarizes the results of the nucleation experiments. Figure 3a shows that the time dependence of the average number of crystals nucleated in one droplet is linear, confirming steady state nucleation. Another important result is that, for all experimental conditions except the highest supersaturation, straight lines pass through the axis origins, indicating that the data are not affected by heterogeneous nucleation.⁹ The presence of crystals at Δt = 0 for a lysozyme concentration of 55 mg/mL indicates that this solution is near its limit of metastability (Figure 1) and nucleation probably occurs during transfer to the incubator, after filling. Thus, in Figure 3b we plot the nucleation rate or nucleation frequency, J . Here, we only need to recall that¹⁶

$$J = K_0 \exp - \left(\frac{16\pi\Omega^2\gamma^3}{3(kT)^3 \ln^2 \beta} \right) \quad (1)$$

where K_0 is a pre-exponential factor, Ω is the volume of a molecule inside the crystal (3.10^{-20} cm³ for tetragonal lysozyme⁹), γ is the crystal–solution interfacial free energy ($J \cdot m^{-2}$), k is the Boltzmann constant (1.3805×10^{-23} J · K⁻¹), T is temperature (K), and β is the

supersaturation, $\beta = C/C_s$, where C is the solution concentration and C_s is the solubility ($C_s = 3.17$ mg/mL in 0.7 M NaCl at pH = 4.5 and $T = 20$ °C¹⁷). From the data presented in Figure 3b we found $\gamma = 0.62$ mJ/m², a value in good agreement with previous determinations from lysozyme nucleation experiments under the same conditions: 0.51–0.64 mJ/m² for the Vekilov group^{9,18} and 0.91 mJ/m² for the Fraden group.¹⁵ Moreover, our kinetic data are also in good agreement with the data of Galkin and Vekilov⁹ obtained for the same NaCl concentration at 12.6 °C (Figure 3b).

3.3. Discussion. The experimental results presented above demonstrate that microfluidics is a direct, accurate, and fast method to measure J . Our results also confirm that at this scale, 250 nL, nucleation kinetics is not affected by volume; that is, to say there are no confined volume effects.^{19,20} As our aim was to obtain reliable statistical data with the minimum quantity of materials, each experimental condition requires only one droplet storage device, i.e. up to 200 droplets, which consumes less than 30 mg of lysozyme for the entire experiments presented here. However, we can expect to measure J in smaller chip channels; for instance, a decrease in channel diameter from 500 to 100 μm decreases droplet volume from 250 nL to 2 nL. In so doing, we would consume no more than 0.3 mg of lysozyme.

Finally, one of the limitations involved in measuring J is the supersaturation range over which the experiment can be performed. When β is too low, heterogeneous nucleation can replace homogeneous nucleation. When β is too high, J is difficult

to measure because it is too rapid. In practice, we are able to measure the nucleation frequency only in the vicinity of the metastable zone limit. In this paper, we show that when experimental volume is diminished, the range of experimentally measurable J is increased. For instance, Galkin and Vekilov⁹ announced a dynamic range of nucleation rates accessible to their technique from ~ 0.7 to ~ 0.007 nuclei/mL·s. Here, with a four times lower volume, we access a range from ~ 3 to ~ 0.3 nuclei/mL·s, thus increasing the supersaturation range experimentally accessible (Figure 3b).

4. CONCLUSIONS

Here we measure lysozyme nucleation kinetics using an easy-to-use and simply constructed microfluidics setup. We confirm that microfluidics is a direct, accurate, and fast method to measure nucleation frequency using only a few milligrams of molecules. Moreover, our microfluidics setup, by diminishing crystallizer volumes, increases the experimental supersaturation range accessible. It would be interesting to test the effect on nucleation of even smaller volumes, as small volume systems offer promising properties.^{19,20}

The advantage of this methodology and setup is its application to all water-soluble molecules, whether mineral, organic, or biological. We are now working on a setup using organic solvents with many potential applications, for instance for pharmaceutical molecules.

AUTHOR INFORMATION

Corresponding Author

*Phone: 336 6292 2866. Fax: 334 9141 8916. E-mail: veesler@cinam.univ-mrs.fr.

ACKNOWLEDGMENT

We thank M. Audiffren (ANACRISMAT) and T. Bactivelane for their technical help. We thank N. Ferte for protein characterization and fruitful discussions. We thank M. Sweetko for English revision.

REFERENCES

- (1) Li, L.; Mustafi, D.; Fu, Q.; Tereshko, V.; Chen, D. L.; Tice, J. D.; Ismagilov, R. F. Nanoliter microfluidic hybrid method for simultaneous screening and optimization validated with crystallization of membrane proteins. *Proc. Natl. Acad. Sci.* **2006**, *103* (51), 19243–19248.
- (2) Shim, J.-U.; Cristobal, G.; Link, D. R.; Thorsen, T.; Fraden, S. Using Microfluidics to Decouple Nucleation and Growth of Protein. *Cryst. Growth Des.* **2007**, *7* (11), 2192–2194.
- (3) Squires, T. M.; Quake, S. R. Microfluidics: Fluid physics at the nanoliter scale. *Rev. Mod. Phys.* **2005**, *77* (3), 977.
- (4) Leng, J.; Salmon, J. B. Microfluidic crystallization. *Lab Chip* **2009**, *9*, 24–34.
- (5) Laval, P.; Salmon, J.-B.; Joanicot, M. A microfluidic device for investigating crystal nucleation kinetics. *J. Cryst. Growth* **2007**, *303*, 622–628.
- (6) Laval, P.; Crombez, A.; Salmon, J.-B. Microfluidic Droplet Method for Nucleation Kinetics Measurements. *Langmuir* **2009**, *25* (3), 1836–1841.
- (7) Ildefonso, M.; Revalor, E.; Punniam, P.; Salmon, J. B.; Candoni, N.; Veesler, S. Nucleation and polymorphism explored via an easy-to-use microfluidic tool. *J. Cryst. Growth* **2011**, article in press.

- (8) Tsekova, D.; Dimitrova, S.; Nanev, C. N. Heterogeneous nucleation (and adhesion) of lysozyme crystals. *J. Cryst. Growth* **1999**, *196* (2–4), 226–233.

- (9) Galkin, O.; Vekilov, P. G. Direct determination of the nucleation rates of protein crystals. *J. Phys. Chem. B* **1999**, *103* (3), 10965–10971.

- (10) Revalor, E.; Hammadi, Z.; Astier, J. P.; Grossier, R.; Garcia, E.; Hoff, C.; Furuta, K.; Okutsu, T.; Morin, R.; Veesler, S. Usual and Unusual Crystallization from Solution. *J. Cryst. Growth* **2010**, *312*, 939–946.

- (11) Anna, S. L.; Bontoux, N.; Stone, H. A. Formation of dispersions using “flow focusing” in microchannels. *Appl. Phys. Lett.* **2003**, *82* (3), 364–366.

- (12) Joanicot, M.; Ajdari, A. Droplet Control for Microfluidics. *Science* **2005**, *309* (5736), 887–888.

- (13) Laval, P.; Giroux, C.; Leng, J.; Salmon, J.-B. Microfluidic screening of potassium nitrate polymorphism. *J. Cryst. Growth* **2008**, *310* (12), 3121–3124.

- (14) Laval, P.; Lisai, N.; Salmon, J. B.; Joanicot, M. A microfluidic device based on droplet storage for screening solubility diagrams. *Lab Chip* **2007**, *7*, 829–834.

- (15) Selimovic, S.; Jia, Y.; Fraden, S. Measuring the Nucleation Rate of Lysozyme using Microfluidics. *Cryst. Growth Des.* **2009**, *9* (4), 1806–1810.

- (16) Boistelle, R.; Astier, J. P. Crystallization mechanisms in solution. *J. Cryst. Growth* **1988**, *90*, 14–30.

- (17) Cacioppo, E.; Pusey, M. L. The solubility of the tetragonal form of hen egg-white lysozyme from pH 4.0 to 5.4. *J. Cryst. Growth* **1991**, *114*, 286–292.

- (18) Galkin, O.; Vekilov, P. G. Are nucleation kinetics of protein crystals similar to those of liquid droplets?. *J. Am. Chem. Soc.* **2000**, *122* (1), 156–163.

- (19) Grossier, R.; Magnaldo, A.; Veesler, S. Ultra-fast Crystallization due to Confinement. *J. Cryst. Growth* **2010**, *312*, 487–489.

- (20) Grossier, R.; Veesler, S. Reaching one single and stable critical cluster through finite sized systems. *Cryst. Growth Des.* **2009**, *9* (4), 1917–1922.